Standard-Compliant HEVC Screen Content Coding for Raw Light Field Image Coding

Sik-Ho Tsang, Yui-Lam Chan, Wei Kuang
Department of Electronic and Information Engineering
The Hong Kong Polytechnic University
Hung Hom, Kowloon, Hong Kong
sik-ho.tsang@polyu.edu.hk, enylchan@polyu.edu.hk, wei.kuang@connect.polyu.hk

***Abstract*— Intra block copy (IBC) in screen content coding (SCC) increases the coding efficiency of screen content (SC) by finding the repeating patterns within the same frame. A raw light field (LF) image contains plentiful repeating patterns since each microlens is capturing the same scene. SCC can be an efficient encoder for LF image compression. Therefore, first, we propose a new LF coding (LFC) model using SCC to encode LF images based on LF image characteristics. Second, a fast IBC search, which is specially designed for light field images, is proposed to reduce the encoder complexity. Experimental results show that our LFC model further improves the coding efficiency of SCC on LF images by 4.87% on average and up to 10.81% bitrate reduction. With our proposed LFC model, the encoded bitstreams are complaint to the SCC standard with even faster decoding time which is user friendly.**

Keywords—HEVC, intra block copy, light field, screen content coding, video coding

I. Introduction

With the facilitation of sensors, computing devices, and 5G networks, it is feasible for the provision of immersive media such as Virtual Reality (VR) and 360-degree videos. Recently, Motion Picture Experts Group (MPEG) has launched the MPEG-I project for the coding representation of immersive media (ISO/IEC 23090) [1]. The goal of MPEG-I to provide users with more degrees of freedom (DoF) to support the current and future VR applications. Particularly, in phase 1b [2] of MPEG-I, limited range of head movement is supported, which is referred as 3DoF+ [3], while in Phase 2 [4], users are allowed to freely move within the immersive environment, i.e. 6DoF [5].

Light field (LF) images [6] have wide range of applications that can be used for 3D object reconstruction to support optical inspection and immersive 360-degree video. Hence, LF is one natural mean to support the immersive applications. LF imaging is an imaging technology which captures a dense number of views in both vertical and horizontal directions. LF images can be acquired by the plenoptic cameras, e.g. Lytro [7] and Raytrix [8], which have a microlens array in front of the imaging sensor. Thus, the captured image is an array of micro images (MIs). There are actually many MIs which capturing the same scene. As a result, many repeating patterns are found within one LF image such as in Fig. 1.

MPEG-I has conducted one of the Exploration Experiments (EEs) for the compression of LF images [9] as shown in Fig. 2. Of the EE for compressions, one is to encode the LF images as a whole, e.g.: [10]. The second way is to decompose LF image into multiview images (or captured by camera array) and then encode the images using multiview video coding (MVC) approach [11]. The third way is to encode 1D image sequence using conventional encoder [12]. Conti *et al.* [10] modified the HEVC encoder to support the self-similarity compensated prediction so as to perform block matching (BM) within the same frame, but bitstream syntax, encoder semantics and memory management for the frame buffer are required to be modified. Consequently, the modified HEVC encoders are not conformed to the standard. And the encoder and decoder complexities are significantly increased by about 8310% and 1190% on average respectively compared with HEVC. When comparing with SCC, the encoder and decoder complexities are also largely increased by about 1450% and 1430% on average respectively. Thus, it is very slow for the encoding process, and it is also inconvenient for end users to acquire a modified non-standard decoder to decode the compressed LF images with slow speed. Alternatively, multiview video coding (MVC) [11] and pseudo video sequence (PVS) [12] approaches convert LF images into a multiview sequence and a pre-defined order sequence respectively. The sequence is then encoded by using MVC encoder or conventional video encoder. It is noted that the MVC and PVS approaches [11]-[12] are focusing on another EE for the compression of LF images after decomposing into multiple images.

In this paper, we focus on the compression for the raw LF image as a whole, and propose to utilize the screen content coding (SCC) [13]-[20] framework for encoding LF images.

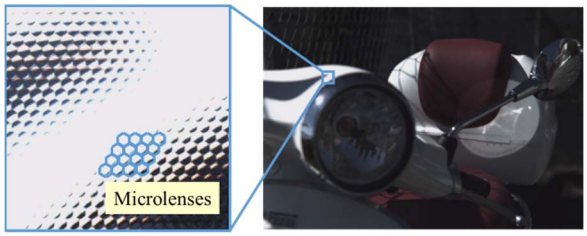

Fig. 1. An example of the light field (LF) image, I05 Vespa.

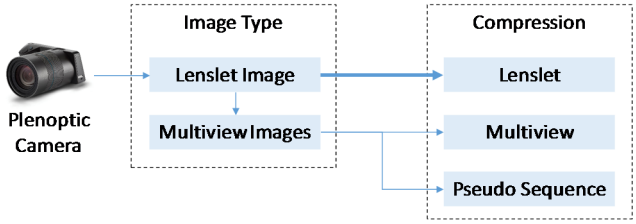

Fig. 2. MPEG-I Activity on the Compression of LF Images.

This work was supported by the Hong Kong Research Grants Council under Research Grant PolyU 152112/17E.

SCC is a recent developed extension profile of High Efficiency Video Coding (HEVC) [21]. Intra block copy (IBC) mode [22]-[24], which is a new coding mode to find the repeating patterns such as text and graphics in computer screen content (SC). With the image characteristics that there are plentiful repeating patterns within the LF images, SCC encoder can be an encoder for encoding LF images as well. However, there are many assumptions or constraints that are based on the SC image characteristics in SCC, which limit the coding performance of LF images. Thereby, we propose to have a new LF coding (LFC) model in SCC encoder to further boost the coding efficiency for LF images. To our best of our knowledge, we believe we are the first to enhance SCC for the coding of LF images. With modifications, our proposed SCC encoder is still definitely conformed to the standard, which means that the bitstreams, encoded by our SCC encoder, are decodable by the standard SCC decoder without any modifications. On top of our new LFC model, we further propose to have a fast IBC search to reduce the complexity.

II. Quick Review on Screen Content Coding

SC images, containing screen captured texts and graphics, have the image characteristics of complex structures with sharp edges which is different from camera-captured images. Conventional intra mode [25], which uses neighbor boundary pixels for prediction, cannot predict them well.

Thereby, two major new modes are introduced to SCC. One is the palette (PLT) mode [26]-[27] which compresses the SC blocks by encoding few base colors and an index map separately, as in Fig. 3(a). PLT is especially useful for blocks with few distinct colors and sharp edges. Another is the intra block copy (IBC) mode [22]-[23] which performs BM to find the repeating patterns within the same frame, as in Fig. 3(b). Different coding unit (CU) and prediction unit (PU) sizes have different searching strategies. Only PU 2N×2N in CU 16×16 (Note that 2N is the size of the current CU.) and PU N×2N in CU 8×8 performs 1D full search to find repeating patterns like vertical edges and texts which are far from the current PU, whereas PU 2N×2N in CU 8×8 and PU 2N×N in CU 8×8 perform 1D local search with search window of 1-CTU (i.e. Coding Tree Unit of size 64×64) height and 2-CTU width. And only PU 2N×2N in CU 8×8 with high CU activity and PU 2N×N in CU 8×8 perform 2D local search with search window of 1-CTU height and 2-CTU width where CU activity, Act, is defined as follows:

$$\begin{aligned} Act &= min(Act_{Hor}, Act_{Ver}) \\ Act_{Hor} &= \sum_{j=0}^{7}\sum_{i=1}^{7}|p(i,j) - p(i-1,j)| \\ Act_{Ver} &= \sum_{j=1}^{7}\sum_{i=0}^{7}|p(i,j) - p(i,j-1)| \end{aligned} \quad (1)$$

where *min(a,b)* is to choose the minimum value of *a* and *b*, and *p(i,j)* is the luminance component of the pixel at the position *(i,j)* in the CU. The reason is that repeating patterns usually have high CU activity such as texts in SC images [23].

In addition, there is a hash search for PU 2N×2N in CU 8×8. Only the candidates with the same hash value as the current PU are searched. The hash value, *H*, is a 16-bit value formed as follows:

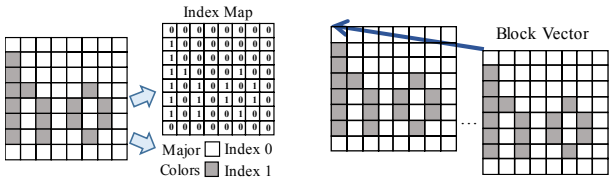

Fig. 3. (a) Palette (PLT) mode, and (b) intra block copy (IBC) mode.

TABLE I. BD-rate (%) and encoding time (%) of SCC with different modes enabled against HEVC

Light Field (LF) Images	SCC (No PLT and IBC)		SCC (Only PLT)		SCC	
	BD-rate	Time	BD-rate	Time	BD-rate	Time
I01 Bikes	0.26	-0.88	0.18	106.37	-12.43	569.10
I02 Danger de Mort	0.22	-1.94	0.23	84.88	-10.06	524.80
I03 Flowers	0.23	-1.07	0.12	107.98	-3.30	452.69
I04 Stone Pillars Outside	0.12	-1.31	0.13	73.73	-3.97	1305.32
I05 Vespa	0.04	-2.22	-0.25	104.09	-20.40	280.45
I06 Ankylosaurus & Diplodocus 1	0.08	-1.22	0.12	78.91	-42.14	288.29
I07 Desktop	0.14	-2.56	-1.69	87.59	-19.41	309.59
I08 Magnet 1	0.10	-2.39	0.09	65.76	-20.07	222.70
I09 Fountain & Vincent 2	0.36	0.47	0.33	89.43	-28.23	1640.21
I10 Friends 1	0.16	-2.63	0.09	71.67	-6.48	251.27
I11 Color Chart 1	0.12	-0.31	0.12	100.37	-43.31	785.19
I12 ISO Chart 12	0.16	-0.88	0.13	84.02	-35.33	852.29
Average	0.16	-1.41	-0.03	87.90	-20.43	623.49

$$\begin{aligned} H = (MSB_3(DC_0) \ll 13) + (MSB_3(DC_1) \ll 10) \\ +(MSB_3(DC_2) \ll 7) + (MSB_3(DC_3) \ll 4) + MSB_4(Grad) \end{aligned} \quad (2)$$

with the DC_0 to DC_3 are the average luminance intensities of the 4×4 sub-blocks inside the CU 8×8. $Grad$ is the average of horizontal and vertical luminance gradients. And $MSB_m(X)$ is the m most significant bits of X. When $Grad$ is smaller than 5, the CU candidate is not included into the hash list for block matching. It can be explained that $Grad$ has the similar assumption as Act in (1) that repeating patterns tend to have high $Grad$ in SC images. It is noted that IBC search is not performed for CU 64×64 and CU 32×32 since repeating patterns tend to be appeared in small-size CU in SC images. Detailed IBC search can be found in [22]-[23]. But these assumptions and constraints are not suitable for LF images.

Experimental analyses are performed by encoding LF images using the standard SCC encoder, HEVC Test Model Version 16.17 Screen Content Model Version 8.6 (HM-16.17+SCM-8.6) [28] according to all intra (AI) configuration in common test condition (CTC) [29] with quantization parameters (QPs) of 22, 27, 32 and 37. The LF images are from [30] with the resolution of 7728×5368. Table I tabulates Bjontegaard delta bitrate (BD-rate) [31] and encoding time of SCC with different modes enabled in percentage compared with HEVC. It can be observed that for SCC with PLT and IBC disabled, i.e. SCC (No PLT and IBC), BD-rate is increased by 0.16% on average with 1.41% decrease in encoding time which is only a small difference due to additional signaling bits or some minor changes in SCC. For SCC with only PLT enabled, i.e.

SCC (Only PLT), BD-rate is decreased by 0.03% on average only with 87.90% increase in encoding time. This is expected since PLT mode is only efficient for encoding CUs with few distinct colors and sharp edges. Because these CUs are frequently appeared in computer-captured SC images but rarely appeared in camera-captured LF images. For SCC with both PLT and IBC enabled, despite 623.49% increase in encoding time, 20.43% on average and up to 43.31% BD-rate reduction can be achieved. This shows that IBC is a very efficient coding tool for encoding LF images. Therefore, in this paper, we propose to have a LFC model in the SCC encoder to further boost the coding efficiency for LF images while maintaining the standard compliant property. As encoder complexity is high, we also propose a fast IBC search to reduce the complexity of our proposed LFC model.

III. Proposed Light Field Image Coding Model

As the original SCC encoder is designed for SC images, some assumptions and constraints are based on SC image characteristics, as aforementioned, which are not suitable for LF images. Thus, we hereby propose to have a new LF coding (LFC) model which enhances the SCC by removing or modifying the assumptions and constraints which were originally dedicated to SC images.

First, we suggest to skip PLT at all CU levels from 64×64 to 8×8 since CUs with few distinct colors and sharp edges are hardly appeared in LF images due to the existence of sensor noise. This can be reflected by the experimental analysis in Table I that BD-rate cannot be reduced by "SCC (Only PLT)".

Second, IBC was originally applied for CU 16×16 and 8×8 only as repeating patterns tend to occur in small-size CUs for SC images. We propose to have IBC at all CU levels for LF images since repeating patterns can be as large as the MI resolution. An CU which overlapped across multiple MIs can also be chosen IBC as the optimal mode if those MIs are capturing a smooth area as in Fig. 4(b).

Third, since IBC is suggested to be performed at all CU levels, we also suggest enabling IBC at all kinds of PUs, i.e. PU 2N×2N, 2N×N and N×2N at all CU levels to further boost the coding efficiency for LF images.

Moreover, as mentioned, searching strategies are varied at different CU and PU sizes due to the SC image characteristics. Instead, we propose to disable 1D full search for all kinds of PUs at all CU levels. This is because the object to be searched in the current MI only occurs at nearby MIs. That means the repeating pattern only occurs close to the current PU to be searched. An example is illustrated in Fig. 4(c), the water splash in a MI can only be searched at nearby MIs but not MIs by far. Therefore, 1D full search is not necessary. Instead, only 1D local search following 2D local search are suggested to be used for IBC. And the constraints in (1), in which only PU 2N×2N in CU 8×8 with high CU activity can perform 2D local search, is also suggested to be removed. Because no matter the CU is with high or low activity in the current MI, it must also appear at nearby MIs.

Last but not least, the search area used for 1D and 2D local searches in the conventional SCC only covers the current and left CTUs. Though the repeating pattern only occurs nearby the current PU, the repeating patterns can still be outside this small

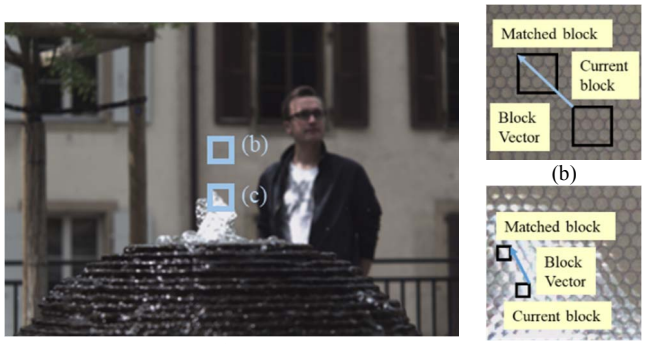

Fig. 4. Illustrative examples of LF image characteristics: (a) An LF image, I09 Fountain & Vincent 2, (b) CU overlapping across multiple MIs with smooth area, and (c) repeating patterns that only occur at nearby MIs.

search area for LF images. And it is meaningless to have search area of the current and left CTUs for CU 64×64 because the current CU already covers the whole current CTU and remains one searching candidate at the left CTU. Thus, we suggest enlarging the search area for 1D and 2D local searches by extending n_y and n_x pixels vertically to the top and horizontally to the left respectively. In particular, our implementation allows a search area of 3-CTU height and 3-CTU width which is a square search area, i.e. n_y=128 and n_x=64.

With the above suggestions based on the LF image characteristics, the proposed LFC model using SCC encoder can further improve the coding efficiency, in which experimental results are shown in Section V, while the encoded bitstreams are still conformed to the standard.

IV. Proposed Fast IBC Search

As aforementioned, the LF image characteristics is different from SC image that the repeating patterns appearing within the current MI only appears again at nearby MIs. And the ranges of CU levels, PU sizes and search area are largely broadened for LF images. Computational complexity is high for our proposed LFC model. Thereby, in this section, we propose a fast IBC search so as to reduce the computational complexity.

Within IBC, for each searching point, the corresponding BM cost, *J(bv)*, is estimated as follows:

$$J(bv) = SAD(Blk_{Cur}, Blk_{bv}) + \lambda \times R(bv) \quad (3)$$

where $SAD(Blk_{Cur}, Blk_{bv})$ is the sum of absolute different (SAD) between the current block, Blk_{Cur}, and the matched block, Blk_{bv}, pointed by the block vector bv, with λ and $R(bv)$ are the Lagrange multiplier and the coding rate of bv respectively. The matched block pointed by bv with the least BM cost $J(bv)$ is selected as the optimal block:

$$bv^* = arg\ min\big(J(bv)\big) \quad (4)$$

where bv^* is the bv of the optimal block. To find the optimal block faster, we propose to have 1D local search only for CU 64×64 and 32×32 in order to reduce the number of BM cost computation in (4) for large-size CUs as it is most likely used

for searching smooth areas which across multiple MIs as in Fig. 4(b).

For small-size CUs, i.e. CU 16×16 and 8×8, in 1D local and 2D searches, a fast hash search is proposed for LF images for different PU sizes. Only the PU candidates with the same hash value with the current PU are searched. The hash values, $H_{2N\times 2N}$, $H_{2N\times N}$ and $H_{N\times 2N}$ for PU 2N×2N, 2N×N and N×2N respectively are as follows:

$$\begin{aligned} H_{2N\times 2N} &= (MSB_m(DC_0) \ll 3m) + (MSB_m(DC_1) \ll 2m) \\ &\quad +(MSB_m(DC_2) \ll m) + MSB_m(DC_3) \\ H_{2N\times N} &= (MSB_m(DC_k) \ll m) + MSB_m(DC_{k+2}) \\ H_{N\times 2N} &= (MSB_m(DC_k) \ll m) + MSB_m(DC_{k+1}) \end{aligned} \quad (5)$$

where k can be 0 or 1 for PU 2N×N and PU 2N×N according to the PU index. It can be seen that the term $Grad$ in (2) is removed. Unlike repeating patterns in SC images that they tend to have high gradient values such as texts, the occurrence of repeating patterns in LF images is due to the fact that neighbor microlenses are capturing the same object. Thereby, only DC values are used for hash estimation. With larger m, fewer PU candidates would be included since the condition of hash matching is stricter. Conversely, with smaller m, more PU candidates would be included. In practice, a bottom-up approach is used for the estimation of DC from 4×4 to 8×8 in order to reduce the hash computation overhead. The optimum value determination of m is mentioned in the next section. Therefore, we make use of LF image characteristics to speed up the coding of large CUs and small CUs.

V. Experimental Results

To evaluate the performance of the proposed techniques, we have performed simulations using the HEVC reference software HM-16.17+SCM-8.6 [28] with the coding conditions [29] and the LF images [30] mentioned in Section II. For the sake of simplicity, the conventional HEVC and SCC encoders are denoted as HEVC and SCC respectively. Our proposed LFC model is denoted as LFC whereas our proposed LFC model with fast IBC search is denoted as "FastLFC(m_{16},m_8)" where m_{16} and m_8 are the values of m in (5) for CU 16×16 and 8×8 respectively. The experiments were conducted on the Dell Precision T1700 computer with an Intel i7-4770 3.40GHz processor and 16GB memory.

Table II tabulates the average BD-rate [31] and the average encoding time obtained by our proposed LFC model with different values of m_{16} and m_8 compared with the conventional SCC. Without fast IBC search, our proposed LFC model obtains 4.87% average BD-rate reduction but also with 97.42% increase in encoding time on average. With m_{16} = 1 and m_8 = 3, FastLFC(1,3), which is our proposed LFC model with fast IBC search, obtains 3.53% average BD-rate reduction and only 57.96% of average increase in encoding time. We chose the case of m_{16} = 1 and m_8 = 3, i.e. FastLFC(1,3), as optimum by considering that it can have a better balance between BD-rate and encoding time.

Table III tabulates the BD-rate and the encoding time obtained by our proposed LFC models compared with the conventional SCC for each individual LF image. It can be seen that our proposed LFC model can obtain up to 10.80% BD-rate reduction for I06 LF image and 4.87% average BD-rate reduction, which is a substantial improvement. Though 97.42% increase in encoding time is obtained, large BD-rate reduction is obtained which indicates that there is still room to improve SCC. Thus, the computational complexity brought by our LFC model is necessary. It is essential to recap that SCC has already obtained up to 43.31% and 20.43% average BD-rate reduction against HEVC as in Table I and we further improve the conventional SCC. This shows that by considering the LF image characteristics, our proposed LFC model can be an efficient coding model for compressing LF images. With our fast IBC search, FastLFC(1,3), we still can obtain up to 9.25% BD-rate reduction for I06 LF image and 3.53% average BD-rate reduction with the increase in encoding time reduced from 97.42% to 57.96%. The searching point reduction by FastLFC(1,3) is also studied that 45.16% of average searching point reduction is obtained compared with LFC. This demonstrates that FastLFC(1,3) has reduced the number of BM cost computation in (4) by 45.16% while still keeping the high coding efficiency.

FastLFC(1,3) is designed based on the characteristics of LF images. To show the effectiveness of FastLFC(1,3), FastLFC(1,3) is also compared with the fast SCC approaches [32]-[33] by deploying them on top of our LFC model, which are denoted as LFC+[32] and LFC+[33] respectively. [32] skips IBC search when the current CU has zero CU activity in (1), or the number of high-gradient pixels is few since repeating patterns are assumed to be rarely occurred in SC images when there is no sharp edges or complex structure. [33] uses machine learning based decision tree to have fast mode decision in SCC. Table IV tabulates the average BD-rate and the encoding time

TABLE II. BD-RATE (%) AND ENCODING TIME (%) OF THE PROPOSED LFC MODELS WITH VARIOUS VALUES OF M_{16} AND M_8 AGAINST SCC.

Approaches	LFC	FastLFC (1,1)	FastLFC (2,1)	FastLFC (1,2)	FastLFC (2,2)	FastLFC (1,3)	FastLFC (2,3)
BD-rate	-4.87	-3.98	-3.47	-3.71	-3.32	-3.53	-3.01
Time	97.42	73.28	68.36	65.71	60.85	57.96	57.55

TABLE III. BD-RATE (%) AND ENCODING TIME (%) OF THE PROPOSED LFC MODELS AGAINST SCC.

Images	**LFC**		**FastLFC(1,3)**		**Images**	**LFC**		**FastLFC(1,3)**	
	BD-rate	**Time**	**BD-rate**	**Time**		**BD-rate**	**Time**	**BD-rate**	**Time**
I01	-4.09	90.55	-2.22	51.66	I07	-2.02	117.83	-0.84	65.84
I02	-4.25	96.52	-2.69	58.45	I08	-7.35	135.35	-5.82	86.99
I03	-1.87	127.61	-0.66	75.60	I09	-3.08	28.17	-1.77	16.99
I04	-1.39	52.63	-0.99	30.79	I10	-2.62	191.23	-1.58	115.11
I05	-6.99	124.33	-5.08	72.71	I11	-6.93	40.11	-5.65	23.44
I06	-10.80	125.40	-9.25	75.84	I12	-7.07	39.30	-5.79	22.16
Average (I01 – I12)						-4.87	97.42	-3.53	57.96

TABLE IV. AVERAGE (I01-I12) BD-RATE (%) AND ENCODING TIME (%) OF VARIOUS APPROACHES AGAINST LFC AND LFC.

Approaches	**Compared to SCC**		**Compared to LFC**	
	BD-rate	**Time**	**BD-rate**	**Time**
LFC	-4.87	97.42	-	-
FastLFC(1,3)	-3.53	57.96	1.43	-18.78
LFC+[32]	6.71	-49.27	12.63	-71.81
LFC+[33]	0.66	33.50	5.81	-28.50

TABLE V. AVERAGE DECODING TIME IN SECONDS (SEC) AND IN PERCENTAGE (%) OF THE PROPOSED LFC MODELS AGAINST SCC.

Approaches	SCC	LFC	FastLFC(1,3)	Conti's [10]
Decoding Time (sec)	2.84	2.70	2.71	43.45 (estimated)
Decoding Time (%)	-	-4.75	-4.46	1430

obtained against SCC and LFC respectively. Our FastLFC(1,3) obtains only 1.43% BD-rate increase on average with 18.78% average encoding time reduction against LFC while LFC+[32] and LFC+[33] obtain 12.63% and 5.81% BD-rate increase on average though with 71.81% and 28.50% average encoding time reduction respectively. By comparing with the conventional SCC, LFC+[32] and LFC+[33] actually have worse coding performance which obtain 6.71% and 0.66% increase in BD-rate on average respectively, even LFC+[32] has 49.27% average encoding time reduction. This is because many low-gradient or low-variance CUs skipped IBC. However these contents in LF images would be definitely appeared again in neighbor microlenses, or an CU overlapping across multiple MIs which capturing the smooth area. They should be encoded by IBC but wrongly skipped. Thus, the BD-rate is increased largely due to misclassification. On the other hand, our FastLFC(1,3) using the hash checking does not include the gradient term, and only involves the average values of sub-blocks as in (5). Therefore, our fast IBC search approach has a better tradeoff on the coding performance and the encoding speed due to the consideration of LF image characteristics.

Moreover, bitstreams encoded by our proposed LFC models can be decoded by the standard SCC decoder we evaluate the decoding time in seconds and in percentages of our proposed LFC models against SCC as shown in Table V. As the decoding process is fast, we decode each image per QP for five times and take the average. For the conventional SCC, it takes 2.84 seconds on average to decode a LF image. And our proposed LFC and FastLFC(1,3) take 2.70 and 2.71 seconds on average which have 4.75% and 4.46% decoding time reduction respectively compared with the conventional SCC. This can be explained that by using our proposed LFC models, there are more large-size CUs using IBC and fewer CUs using the conventional intra mode. More large-size CUs means that the time of recursive quad-tree decoding down to small-size CU is saved and the number of times for motion compensation is reduced. Compared with [10] which has 1430% increased decoding time by a modified decoder, ours are much user friendly for end users to decode the raw 7728×5368 LF images at fast speed by using a standard SCC decoder.

VI. CONCLUSIONS

Intra block copy (IBC) is a new coding tool in screen content coding (SCC) for encoding repeating patterns within the screen content (SC) image. It can be a potential tool for encoding light field (LF) image as well since an object captured in one micro image (MI) can be found at nearby MIs. Therefore, in this paper, we propose to have a new LF coding (LFC) model for coding LF images by enhancing the SCC encoder based on the LF image characteristics which obtains up to 10.81% and 4.87% average BD-rate reduction. (The term "LFC" is a tribute to my favorite Liverpool Football Club and the sixth European Cup.) In addition, we propose a fast IBC search to reduce the computational complexity. Moreover, the encoded bitstreams are still totally decodable by the conventional SCC decoder. We are the first to modify the SCC platform for the development of LF coding. By widening the application of SCC encoder using our proposed LFC model, it is strongly recommended for usage and development so that the SCC encoder not just only encodes SC images, but also encodes LF images. And it is even possible to develop a LFC profile for compressing the LF images.

REFERENCES

[1] MPEG-I: Coded Representation of Immersive Media. Available: https://mpeg.chiariglione.org/standards/mpeg-i.

[2] "Requirements MPEG-I Phase 1b," ISO/IEC JTC1/SC29/WG11 MPEG, document N17331, Gwangju, South Korea, Janaury 2018.

[3] "MPEG-I Phase 1 Use Cases (v1.5)," ISO/IEC JTC1/SC29/WG11 MPEG, document N17886, Ljubljana, Slovenia, July 2018.

[4] "Requirements MPEG-I Phase 2," ISO/IEC JTC1/SC29/WG11 MPEG, document N18127, Marrakech, Morocco, January 2019.

[5] "MPEG-I Phase 2 Use Cases," ISO/IEC JTC1/SC29/WG11 MPEG, document N17932, Macao, China, October 2018.

[6] T. Georgiev, and A. Lumsdaine, "Focused plenoptic camera and rendering," *J. Electron. Imag.*, Vol. 19, no. 2, 021106, pp. 1-11, April 2010.

[7] R. Ng, "Digital Light Field Photography", *Doctoral Thesis*, Stanford University, 2006.

[8] Raytrix Website [Online]. Available: https://raytrix.de/.

[9] "Exploration Experiments for MPEG-I: Compression of Dense Representation of Light Fields," *MPEG-I*, MPEG2018/N17723, Ljubljana, Slovenia, July 2018.

[10] C. Conti, P. Nunes, and L. D. Soares, "Light Field Image Coding with Jointly Estimated Self-Similarity Bi-Prediction," *J. Signal Process.: Image Comm.*, Vol. 60, pp. 144-159, February 2018.

[11] G. Wang, W. Xiang, M. Pickering, and C. W. Chen, "Light Field Multi-View Video Coding With Two-Directional Parallel Inter-View Prediction," *IEEE Trans. Image Process.*, vol. 25, no. 11, pp. 5104-5117, Nov. 2016.

[12] D. Liu, L. Wang, L. Li, Z. Xiong, F. Wu, and W. Zeng, 'Pseudo-Sequence-Based Light Field Image Compression', *Proc. Int. Conf. Multimed. Expo Work*., pp. 1-4, Seattle, U.S.A., July 2016.

[13] J. Xu, R. Joshi, and R. A. Cohen, "Overview of the Emerging HEVC Screen Content Coding Extension," *IEEE Trans. Circuits Syst. Video Technol.*, vol. 26, no. 1, pp. 50-62, January 2016.

[14] S.-H. Tsang, Y.-L. Chan, and W.-C. Siu, "Fast and Efficient Intra Coding Techniques for Smooth Regions in Screen Content Coding Based on Boundary Prediction Samples," *Proc. Int. Conf. Acoustics, Speech Signal Process. (ICASSP)*, pp. 1409-1413, Brisbane, Australia, April 2015.

[15] S.-H. Tsang, Y.-L. Chan, and W. Siu, "Hash Based Fast Local Search for Intra Block Copy (IntraBC) mode in HEVC Screen Content Coding," *Proc. APSIPA Annual Summit and Conf. (APSIPA ASC)*, pp. 396-400, Hong Kong, China, December 2015.

[16] W. Kuang, S.-H. Tsang, Y.-L. Chan, and W.-C. Siu, "Fast Mode Decision Algorithm for HEVC Screen Content Intra Coding," *Proc. IEEE Int. Conf. Image Process. (ICIP)*, pp. 2473-2477, Beijing, China, September 2017.

[17] S.-H. Tsang, Y.-L. Chan, W. Kuang, and W.-C. Siu, "Reduced-Complexity Intra Block Copy (IntraBC) Mode With Early CU Splitting and Pruning for HEVC Screen Content Coding," *IEEE Trans. Multimedia*, vol. 21, no. 2, pp. 269-283, February 2019.

[18] W. Kuang, Y.-L. Chan, S.-H. Tsang, and W.-C. Siu, "DeepSCC: Deep learning based fast prediction network for screen content coding," *IEEE Trans. Circuits Syst. Video Technol.*, early access, 2019.

[19] S.-H. Tsang, Y.-L. Chan, and W. Kuang, "Mode Skipping for HEVC Screen Content Coding via Random Forest," *IEEE Trans. Multimedia*, vol. 21, no. 10, pp. 2433-2446, October 2019.

[20] W. Kuang, Y.-L. Chan, S.-H. Tsang, and W.-C. Siu, "Online-Learning-Based Bayesian Decision Rule for Fast Intra Mode and CU Partitioning

Algorithm in HEVC Screen Content Coding," *IEEE Trans. Image Process.*, vol. 29, no. 1, pp. 170-185, January 2020.

[21] G. J. Sullvian, J. Ohm, W.-J. Han, and T. Wiegand. "Overview of the High Efficiency Video Coding (HEVC) Standard," *IEEE Trans. Circuits Syst. Video Technol.*, vol. 22, no. 12, pp. 1649-1668, December 2012.

[22] X. Xu, S. Liu, T.-D. Chuang, Y-W. Huang, S.-M. Lei, K. Rapaka, C. Pang, V. Seregin, Y.-K. Wang, and M. Karczewicz, "Intra Block Copy in HEVC Screen Content Coding Extensions," *IEEE J. Emerging Selected Topics Circuits Syst.*, vol. 6, no. 4, pp. 409-419, December 2016.

[23] M. Budagavi, and D.-K. Kwon, "Fast Intra Block Copy (IntraBC) Search for HEVC Screen Content Coding," *Proc. IEEE Int. Symp. Circuits Syst. (ISCAS)*, pp. 9-12, Melbourne, Australia, June 2014.

[24] S.-H. Tsang, W. Kuang, Y.-L. Chan, and W.-C. Siu, "Decoder Side Merge Mode and AMVP in HEVC Screen Content Coding," *Proc. IEEE Int. Conf. Image Process. (ICIP)*, pp. 260-264, Beijing, China, September 2017.

[25] J. Lainema, F. Bossen, W.-J. Han, J. Min, and K. Ugur, "Intra Coding of the HEVC Standard," *IEEE Trans. Circuits Syst. Video Technol.*, vol.22, no.12, pp. 1792-1801, December 2012.

[26] W. Pu *et al.*, "Palette Mode Coding in HEVC Screen Content Coding Extension," *IEEE J. Emerging Selected Topics Circuits Syst.*, vol. 6, no. 4, pp. 420-432, December 2016.

[27] S.-H. Tsang, Y.-L. Chan, and W.-C. Siu, "Exploiting inter-layer correlations in scalable HEVC for the support of screen content videos," *Proc. Int. Conf. Digital Signal Process.*, pp. 888-892, Hong Kong, China, August 2014.

[28] HM-16.17+SCM-8.6, HEVC Test Model Version 16.17 Screen Content Model Version 8.6 [Online]. Available: https://hevc.hhi.fraunhofer.de/svn/svn_HEVCSoftware/tags/HM-16.17+SCM-8.6/.

[29] "Common Test Conditions for Screen Content Coding," *JCT-VC*, JCTVC-U1015, Warsaw, Poland, June 2015.

[30] M. Rerabek, T. Bruylants, T. Ebrahimi, F. Pereira, and P. Schelkens, "ICME 2016 Grand Challenge: Light-Field Image Compression Call for Proposals and Evaluation Procedure," Seattle, U.S.A., July 2016.

[31] G. Bjontegaard, "Calculation of Average PSNR Differences Between RD Curves," *VCEG*, VCEG-M33, Austin, U.S.A., April 2001.

[32] S.-H. Tsang, W. Kuang, Y.-L. Chan, and W.-C. Siu, "Fast HEVC Screen Content Coding By Skipping Unnecessary Checking of Intra Block Copy Mode Based on CU Activity and Gradient," *Proc. APSIPA Annual Summit and Conf. (APSIPA ASC)*, pp. 1-5, Jeju, Korea, December 2016.

[33] H. Yang, L. Shen, and P. An, "An Efficient Intra Coding Algorithm Based on Statistical Learning for Screen Content Coding," *Proc. IEEE Int. Conf. on Image Process. (ICIP)*, pp. 2468-2472, Beijing, China, September 2017.